Prevalence of Fission and Evaporation in the Decay of Heavy Nuclei Excited up to 1000 MeV with Energetic Antiprotons

U. Jahnke,[1,3] W. Bohne,[1] T. von Egidy,[2] P. Figuera,[1] J. Galin,[3] F. Goldenbaum,[1] D. Hilscher,[1] J. Jastrzebski,[4] B. Lott,[3] M. Morjean,[3] G. Pausch,[5] A. Péghaire,[3] L. Pienkowski,[4] D. Polster,[1] S. Proschitzki,[6] B. Quednau,[3] H. Rossner,[1] S. Schmid,[2] and W. Schmid[2]

[1]*Hahn-Meitner-Institut Berlin, Glienickerstrasse 100, D-14109 Berlin, Germany*
[2]*Technische Universiät München, D-85748 Garching, Germany*
[3]*GANIL(IN2P3-CNRS,DSM-CEA), BP 5027, F-14076 Caen Cedex 05, France*
[4]*Heavy Ion Laboratory, Warsaw University, 02-093 Warszawa, Poland*
[5]*FZ-Rossendorf, D-01314 Dresden, Germany*
[6]*IPN Orsay, BP 1, F-91406 Orsay Cedex, France*

(Received 23 April 1999)

Annihilation of 1.2 GeV antiprotons has been explored as a means to generate high thermal excitation in heavy nuclei (U, Au, Ho) and to observe their decay with a minimal contribution from dynamical distortion. Conventional fission and heavy residue formation are found to dominate the decay up to $E^* \approx 1000$ MeV. Both modes are increasingly accompanied by a modest emission of intermediate-mass fragments (up to 1 on average), but true multifragmentation is not observed. These features are in agreement with the predictions of the statistical model with no need for a fission delay $\tau_f > 0.5 \times 10^{-21}$ s.

PACS numbers: 25.43.+t, 24.60.Dr, 24.75.+i

Evaporation and fission are the dominant decay mechanisms of heavy nuclei in the low-energy regime, well documented as a function of excitation energy E^* up to about 200 MeV. At higher excitation, one expects [1–3] more diverse decay modes to become accessible to the nucleus: multibody fragmentation with the emission of intermediate-mass fragments (IMFs) and—when the excitation exceeds notably the binding energy of the nucleus—also vaporization into single nucleons or very light nuclei. It is these novel [4] and relatively scarce [5] decay modes which have recently received much attention. The evolution with excitation energy of the dominant reaction channels as well as the conventional decay branches, heavy evaporation residue (HR) production and fission, instead has not—with a few exceptions in light-ion [6] and heavy-ion reactions [7,8]— been pursued to higher excitation energy. It is one of the goals of this investigation to fill this gap and to provide a complete balance of all important decay channels as a function of E^*.

The other aspect which distinguishes the present investigation from most of the others is the choice of the reaction for the excitation. This is an important issue because, at high excitation, formation of the hot nucleus and its decay are no longer detachable, but are interconnected in time scale and by dynamical distortions. Indeed, shape distortions, rotation, and in particular compression of the nucleus could have a similar strong effect on its fragmentation as purely thermal excitation [9]. Their influence on the decay is surely an important experimental objective. We believe, however, that the knowledge of the purely statistical decay mechanisms is a prerequisite to it. Collective excitations are generally believed to be more strongly induced in heavy-ion reactions, while light projectiles create incoherent thermal excitations. For this reason we have chosen annihilation of energetic antiprotons ($\overline{p}$) as the closest approach to purely thermal excitation, eventually even better or "softer" than excitation with GeV protons.

The picture of the $\overline{p}$-nucleus reaction [10,11] at 1.2 GeV kinetic energy is, in a few words, the $\overline{p}$ annihilates on a nucleon at the outskirts of the nucleus or deeper inside for a smaller impact parameter, thereby creating five pions on the average with a mean energy of 450 MeV. Part of these pions penetrate into the nucleus and mediate its heating in a radiationlike way by creating several intranuclear cascades (INCs). The whole excitation and equilibration is faster (30 fm$/c$ or 10^{-22} s) than in heavy-ion reactions. It leaves the nucleus relatively intact with a broad excitation energy distribution extending up to 1000 MeV and with a maximum loss of about 22 units in mass, 6 units in charge, and modest angular momenta up to $25\hbar$ at the highest E^*. The details of this fast reaction step are reliably modeled by INC codes [10,11].

Our experimental method has the following basic features: Each incoming $\overline{p}$ is tagged with a start detector, each reaction in the target is recognized with virtually no threshold on inelasticity and all evaporated neutrons, light charged particles (LCPs), as well as IMFs, fission fragments (FFs), and HRs are registered event-by-event with 4π spatial coverage. The latter groups are detected with minimum energy thresholds, at the expense, however, of a superior resolution in A or Z. From the observation of all light particles in the evaporation cascade, we infer the thermal excitation deposited in the target nucleus in each reaction and then deduce the cross

section for the different decay channels as well as their relative weight as a function of excitation energy.

The experiment was performed at LEAR, the low-energy antiproton ring at CERN, consuming about 5×10^5 $\overline{p}$/s of the maximum kinetic energy at LEAR, 1.22 GeV. After tagging the $\overline{p}$'s with a thin plastic detector, 16 m upstream, they were focused onto 1–2 mg/cm^2 thick metallic ^{238}U, ^{197}Au, and ^{165}Ho targets in the middle of the reaction chamber inside the spherical 4π Berlin neutron ball (BNB) with 1500l of Gd loaded scintillator liquid. The chamber also houses around the target the Berlin silicon ball (BSiB), a sphere of 20 cm in diameter built from 158 independent 500-μm-thick Si detectors with a total active area of 92% of 4π. Charged particles are identified in BSiB by means of time-of-flight versus energy correlations with a mass resolution of ± 3 units for $A = 20$ and ± 15 units for $A = 100$, however, with thresholds as low as 1 to 2 MeV. BNB serves as a twofold detector due to its prompt and delayed responses [12]. The prompt scintillation light originates from γ rays, high-energy charged particles, in particular annihilation pions, and recoil protons from scattering of neutrons in the scintillator. It has amplitudes equivalent to 500 MeV or more and indicates unmistakably the occurrence of a reaction. The delayed light response, instead, comes from neutrons which are captured into Gd after moderation and provides the total number of evaporated neutrons.

The first step in the data analysis, which has been described before [13], was the construction of the excitation energy distributions $d\sigma/dE^*$. They exhibit rather broad maxima near 420, 360, and 320 MeV for U, Au and Ho, respectively, and extend up to about 1000 MeV. Moreover, they are in very good agreement with the predictions of the INC model [10] which gives confidence also in the INC predictions of the nucleonic content and the angular and linear momenta of the nuclei after the fast INC stage.

Apart from the LCPs, the charged particle data exhibit the three distinct groups: IMFs, FFs, and HRs. The boundaries between them, however, become more and more blurred with increasing E^*. The basic reason for this is the widening of the mass distribution of FFs and HRs and the enhanced IMF production with increasing E^* and, to some lesser extent, originates also from the use of relatively thick targets, by which we had to compensate for the low available $\overline{p}$ intensity. As far as FFs are concerned, we also found that the traditional criteria for their selection, i.e., the angular correlation between the fragments or the total kinetic energy release, were not helpful, again, because of the dispersion from the strong neutron, LCP, and IMF emission. Therefore the distinction of the groups was based on cuts in mass. More specifically, IMFs were defined by $5 < A < 25$ and the two FFs were selected with the condition $A_1 \geq A_2 \geq 35$, 30, and 25 for U, Au, and Ho, respectively, with A_1 being the heaviest and A_2 the second heaviest mass in the event. For HRs, instead, the criterion $A_2 < 35$ (U), 30 (Au), and 25 (Ho) was used as well as the additional condition that the sum of all detected masses should exceed $0.7A_{\text{target}}$, which ensures the separation from events where only one FF was detected. The mass calibration itself was obtained from the LCP masses and the well-known FF masses from U fission at low excitation.

Figure 1 demonstrates the relative importance of fission and HR production with increasing E^* as seen in the experiment. It shows that the FFs experience a loss in energy with increasing E^* because the INC-related depletion of the target charge weakens the Coulomb repulsion between them. For the HRs the contrary is true: They are hardly detectable due to target thickness effects for $E^* < 250$ MeV (still less for U than for Au) but gain in energy and become more and more prominent in the higher E^* bins. Where does the recoil come from, which propels the HRs? From the $\overline{p}$ annihilation with the pions as an intermediary, one expects a diffuse momentum transfer in all directions with a moderate mean of only 0.2 GeV/c in beam direction. However, the small initial momenta can be strongly increased (not on average, but in the wings of the distribution) by the subsequent statistical evaporation chain from up to 60 particles or the fluctuations therein, as seen from the left panels in Fig. 2. They show the invariant cross section of α particles relative to the velocity direction of the cascade nucleus (reconstructed here for simplicity not directly from the HRs but from the FF velocity vectors). The α particles are preferentially emitted opposite to the direction of the cascade nucleus, thereby reinforcing its momentum and energy.

The right panels in Fig. 2 concern the time scale of fission. The parallel and perpendicular velocity components of the α's are plotted here in the scission frame, where the heavier FF moves towards 0° (positive direction) and the lighter FF moves backwards to 180°, with their proper velocity distributions indicated by the histograms. The important feature in this graph is that the tips of the α-velocity vectors are concentrated uniformly close to a single ring about the origin, indicating emission from the

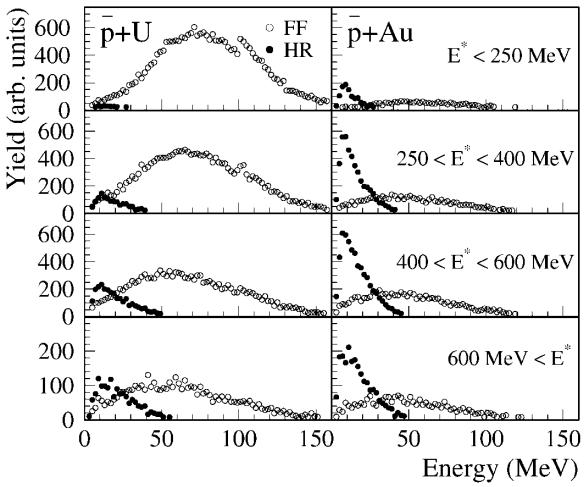

FIG. 1. Kinetic energy spectra of FFs (open dots) and HRs (black dots) from $\overline{p}$ + U and Au for four indicated bins in E^*.

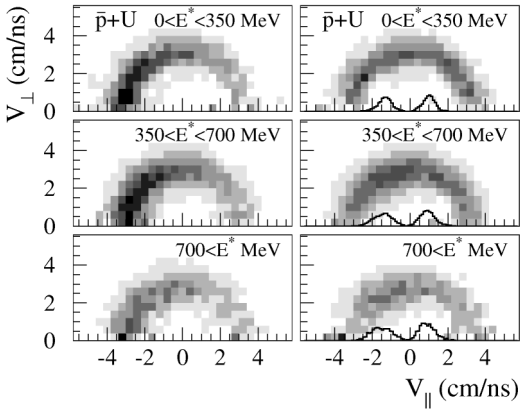

FIG. 2. Invariant cross sections (in relative units) of α particles from $\overline{p}$ + U for three bins in E^*. The left panels show the laboratory velocity components $v_\perp$ and $v_\parallel$ of the α particles relative to the recoil direction of the fissioning nucleus ($+v_\parallel$) and the right panels refer to the scission frame, where the heavier FF moves towards $+v_\parallel$ and the lighter FF moves to $-v_\parallel$ with their velocity distributions indicated by the histograms.

composite system. Emission from the FFs, instead, would have manifested itself by a gathering on two circles about the centers of the histograms, with somewhat smaller radii resulting from lower Coulomb repulsion. The message from this plot is that most of the evaporation precedes scission, or that the total fission process is slow and the FFs are relatively cold at scission. Such a conclusion has been reached before on a more quantitative level at lower E^* [14]; here, however, it is important that fission retains this singularity up to much higher E^*.

Besides HRs and FFs the third mass group which deserves particular attention in the context of multifragmentation is the IMFs, or rather the event group with IMFs as the heaviest detected fragments. The question is whether these events stem from true multifragmentation, i.e., the complete fragmentation solely into IMFs and light particles, or are only the remnants from events where heavier masses have eluded detection. The multiplicity M_{IMF} of IMFs in this group extends up to 5 or 6, but the average of the Poisson-like distribution is rather low and within the error bars not discernible from that of all events, which is considered as a function of E^* in Fig. 3. $\langle M_{\mathrm{IMF}}\rangle$ increases slowly with E^* and approaches about 1 at the highest E^*, which is quite consistent with a somewhat larger $\langle M_{\mathrm{IMF}}\rangle$ observed in other light-ion reactions at higher energy [15,16]. With a mean IMF mass of 9 to 10 units the sum mass of all IMFs in either group is at best 50 to 60 units and thus remains far below the values which can be expected (with respect to the good IMF detection efficiency of 70%–80%) for true multifragmentation. In the same Fig. 3 we also display the mean IMF abundance in the FF-event group. Fission seems to have (more obvious for U than for Au) relatively fewer IMFs in common, which we attribute to the reduction of fissility following the emission of an IMF.

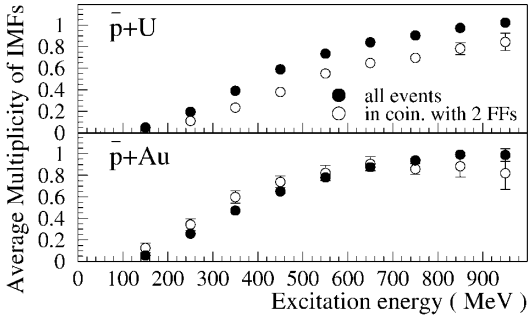

FIG. 3. Average multiplicity (corrected for detector acceptance ϵ_{IMF}) of IMFs (with $5 < A < 25$) from $\overline{p}$ + U, Au as a function of E^*, as observed in all events (black dots) or in coincidence with two FFs (open dots).

In order to deduce the probability of fission $P_f(E^*)$ or HR production $P_{\mathrm{HR}}(E^*)$ as a function of E^*, we have estimated the respective detection efficiencies. We do so for the FFs by simulating the whole two-step INC plus evaporation process with the INC code [10] coupled to a statistical model (SM) code (GEMINI [17]) and considering the energy loss and straggling in the target foil. The result is that for U the probability to detect both FFs amounts to 0.6 at low E^* and falls to 0.45 at $E^* = 1000$ MeV with an estimated relative uncertainty of $\pm 10\%$; for Au and Ho the values are 0.5 to 0.30 ($\pm 20\%$) and 0.4 to 0.25 ($\pm 30\%$), respectively. For the HRs we estimate the detection efficiency ϵ_{HR}—in an admittedly crude way—from the cascade-nucleus velocity distribution (deduced again from the FF vectors): ϵ_{HR} increases from 0.06 ($\pm 30\%$) at $E^* = 200$ MeV to 0.35 ($\pm 20\%$) at $E^* = 1000$ MeV.

Once the detection efficiency is known we can deduce $P_f(E^*)$ from the yield of events with both FFs detected and $P_{\mathrm{HR}}(E^*)$ from the observed HR yield, both shown in Fig. 4. The error bars stand for the effect of a variation of

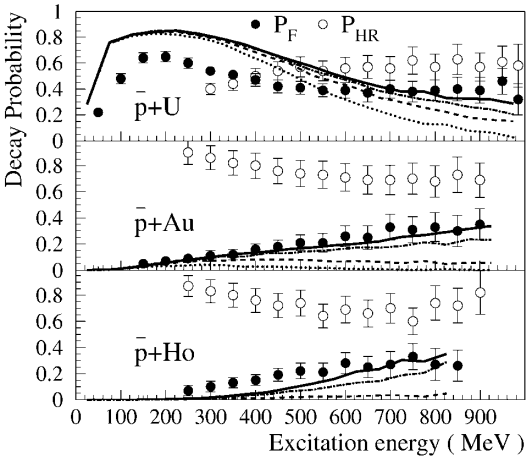

FIG. 4. Probability of fission $P_f(E^*)$ (black dots) and HR production $P_{\mathrm{HR}}(E^*)$ (open dots) observed in $\overline{p}$ + U, Au, and Ho. The lines show the result of SM calculations for $P_f(E^*)$ with $\tau_f = 0$ s (solid line), $\tau_f = 2 \times 10^{-21}$ s (dotted line), 0.5×10^{-21} s (dashed line), and 0.1×10^{-21} s (dotted-dashed line).

the mass cuts in the FF and HR definition by ± 10 units as well as for systematic and statistic errors. The uncertainty introduced by the relatively small HR detection efficiency and their rough estimation would in principle exceed these bars at low E^*. We do, however, have another access for deducing $P_{\mathrm{HR}}(E^*)$ from the before-mentioned group of events with IMFs as the heaviest masses. Since this group does not originate from true multifragmentation as well as the group with exclusively LCPs, we assign them to events where a HR has not been detected and we correct for the low percentage (5% to 15%) of events where both FFs have not been seen. If we then add the events with detected HRs, we arrive directly at a result for $P_{\mathrm{HR}}(E^*)$ which is rather close (and within the uncertainty bars) to the one quoted in Fig. 4.

$P_f(E^*)$ and $P_{\mathrm{HR}}(E^*)$ in Fig. 4 add up closely to 100% up to the highest E^*. True multifragmentation as an independent decay mode, distinct from fission or HR production, is not observed (probability $<10^{-4}$). Multifragmentation with the less stringent but more often used definition [1] $M_{\mathrm{IMF}} \geq 3$ approaches a probability of only about 5% at the highest E^* (it is included in the present analysis in P_f and P_{HR}), which is not surprising, though, because our maximum E^* is still in the region of the expected threshold for this process [1,2].

As the last step, we confront the decay data with predictions of the SM, once more in Fig. 4. For this purpose the SM code GEMINI, provided with standard decay parameters [$a_n = A/10$ MeV^{-1}, $a_f/a_n = 1.00$ (U), 1.022 (Au), and 1.045 (Ho) and Sierk barriers [18] for symmetric fission], has been applied to the whole scope of nuclei emerging from the fast INC excitation [10,13] and the resulting $P_f(E^*)$ is given by the solid lines. We see that the slow and continuous increase of P_f with E^* for Au and Ho as well as of the broad maximum near 200 MeV for U, followed by the considerable decrease of P_f which originates from the depletion of the target nucleus in the INC step is satisfactorily described. This is all the more true as a finer parameter adjustment has not been tried with respect to the many uncertain ingredients in this calculation. HR formation is also the complement to fission in the calculation as it is in the experiment.

Because of the large extension in E^* of the present experiment, $P_f(E^*)$ becomes very sensitive, viz., by more than 1 order of magnitude more than in previous investigations [19], to the issue of the transient time τ_f for fission. This is the time needed to reach the saddle point, where fission is decided upon or where $P_f(E^*)$ is enumerated according to the remaining E^*. An increased τ_f allows for a stronger presaddle evaporation and thus for a stronger reduction in E^* and, consequently, also in $P_f(E^*)$. The broken lines in Fig. 4 show the effect of the introduction of such a delay in the range of $\tau_f = 2$ to 0.1×10^{-21} s and it seems evident that any delay in excess of about 0.5×10^{-21} s would seriously worsen the relatively good agreement with the data at higher E^*. It should, however, be noted that at about $E^* = 500$ MeV the compound nucleus lifetime becomes as short as 10^{-22} s, i.e., as short as the before-mentioned INC-equilibration time, and that therefore the applicability of the SM may become altogether questionable above 500 MeV.

In conclusion, we have observed HR formation and fission in the decay of heavy nuclei as a function of excitation energy up to 1000 MeV, considerably farther than in previous investigations with light projectiles. Both decay modes make up the reaction cross section. At higher excitation they are, on average, accompanied by the emission of up to one IMF, but there is very little margin for true multifragmentation into a larger number of only IMFs and light particles. The $\overline{p}$ excitation supposedly is mostly thermal, free from excessive angular momenta or other collective excitations. The persistence of fission with its inherent slow time scale up to the highest excitations may be taken as the most obvious indication that the nucleus has survived this excitation as a self-bound and dense system, which, however, seems difficult to reconcile with the recent claim [15] of a strong nuclear expansion following ^{3}He-induced reactions. The main features of the evolution of fission and residue production are satisfactorily reproduced by the SM and, as a by-product, we have also shown that, though the total fission time till scission is long [14], the presaddle delay has to be shorter than 0.5×10^{-21} s.

We wish to thank Ye. S. Golubeva and A. S. Iljinov from INR Moscow for providing us with the INC calculations and for many helpful discussions. One of us (U. J.) thanks Ganil for the warm hospitality experienced during a recent stay.

[1] J. P. Bondorf *et al.*, Phys. Rep. **257**, 133 (1995).
[2] D. H. E. Gross, Rep. Prog. Phys. **53**, 605 (1990).
[3] W. A. Friedman, Phys. Rev. C **42**, 667 (1990).
[4] L. G. Moretto and G. J. Wozniak, Annu. Rev. Nucl. Part. Sci. **43**, 379 (1993).
[5] Ch. O. Bacri *et al.*, Phys. Lett. B **353**, 27 (1995).
[6] X. Ledoux *et al.*, Phys. Rev. C **57**, 2375 (1998).
[7] D. Utley *et al.*, Phys. Rev. C **49**, R1737 (1994).
[8] E. Schwinn *et al.*, Nucl. Phys. **A568**, 169 (1994).
[9] L. De Paula *et al.*, Phys. Lett. B **258**, 251 (1991).
[10] Ye. S. Golubeva *et al.*, Nucl. Phys. **A483**, 539 (1988).
[11] J. Cugnon *et al.*, Nucl. Phys. **A484**, 542 (1988).
[12] J. Galin and U. Jahnke, J. Phys. G **20**, 1105 (1994).
[13] F. Goldenbaum *et al.*, Phys. Rev. Lett. **77**, 1230 (1996).
[14] D. Hilscher and H. Rossner, Ann. Phys. (Paris) **17**, 471 (1992).
[15] K. Kwiatkowski *et al.*, Phys. Rev. Lett. **74**, 3756 (1995).
[16] W.-C. Hsi *et al.*, Phys. Rev. Lett. **79**, 817 (1997).
[17] R. J. Charity *et al.*, Nucl. Phys. **A483**, 371 (1988).
[18] A. J. Sierk, Phys. Rev. C **33**, 2039 (1986).
[19] L. G. Moretto *et al.*, Phys. Rev. Lett. **75**, 4186 (1995).